CONF-8908129--1

HEAVY-ION SCATTERING NEAR THE COULOMB BARRIER: SOME RECENT DEVELOPMENTS*,†

CONF-8908129--1

DE89 016849

G. R. Satchler
Oak Ridge National Laboratory
Oak Ridge, TN 37831, U.S.A.

1. THRESHOLD ANOMALIES

1.1 A Brief Review
1.2 Dispersion Relations

1.1.1 Elastic scattering
1.2.2 Nonelastic scattering

2. OPTICAL MODEL FOR FUSION

2.1 Introduction
2.2 The Barrier Penetration Model
2.3 Formal Basis of the Optical Model
2.4 Where Does Fusion Occur?
2.5 Spin Distributions

3. REFERENCES

DISCLAIMER

This report was prepared as an account of work sponsored by an agency of the United States Government. Neither the United States Government nor any agency thereof, nor any of their employees, makes any warranty, express or implied, or assumes any legal liability or responsibility for the accuracy, completeness, or usefulness of any information, apparatus, product, or process disclosed, or represents that its use would not infringe privately owned rights. Reference herein to any specific commercial product, process, or service by trade name, trademark, manufacturer, or otherwise does not necessarily constitute or imply its endorsement, recommendation, or favoring by the United States Government or any agency thereof. The views and opinions of authors expressed herein do not necessarily state or reflect those of the United States Government or any agency thereof.

"The submitted manuscript has been authored by a contractor of the U.S. Government under contract No. DE-AC05-84OR21400. Accordingly, the U.S. Government retains a nonexclusive, royalty-free license to publish or reproduce the published form of this contribution, or allow others to do so, for U.S. Government purposes."

*To be presented at XII Workshop on Nuclear Physics, Iguazú Falls, Argentina, August 28 - September 1, 1989.

†Research sponsored by the Division of Nuclear Physics, U.S. Department of Energy under contract No. DE-AC05-84OR21400 with Martin Marietta Energy Systems, Inc.

DISTRIBUTION OF THIS DOCUMENT IS UNLIMITED

MASTER

HEAVY-ION SCATTERING NEAR THE COULOMB BARRIER: SOME RECENT DEVELOPMENTS

G. R. Satchler
Oak Ridge National Laboratory
Oak Ridge, TN 37831, U.S.A.

1. THRESHOLD ANOMALIES

1.1 A Brief Review

The term "threshold anomaly" (TA) refers to the rapid, localized variation of the heavy-ion optical potential $U(E) = V(E) + iW(E)$ with energy E at low energies in the vicinity of the top of the Coulomb barrier. (The corresponding Fermi-surface anomaly for nucleons[1)] has been known for a long time.) The main features are that the strength of the imaginary potential, in the surface region to which the elastic scattering is sensitive, increases rapidly as the energy rises above the Coulomb barrier and then saturates at a more-or-less constant value, while at the same time the real, attractive potential in the same region decreases rapidly and then remains more-or-less constant. The behavior of the absorptive potential W(E) is easy to understand because the Coulomb barrier effectively closes the nonelastic channels at the lower energies, but increasing the energy above the barrier allows absorption to take place. Hence the word "threshold". The term "anomaly" applies to the real potential V(E), whose behavior was unexpected. Figure 1 shows the canonical example.[2)]

A number of other cases have been seen; Fig. 2 is a recent example.[3)] However, obtaining similar data for heavy systems remains an experimental challenge because of resolution problems.

The above explanation for W(E) implies that the behavior seen is a coupled-channels (CC) effect, and this has been confirmed[4,5)] by

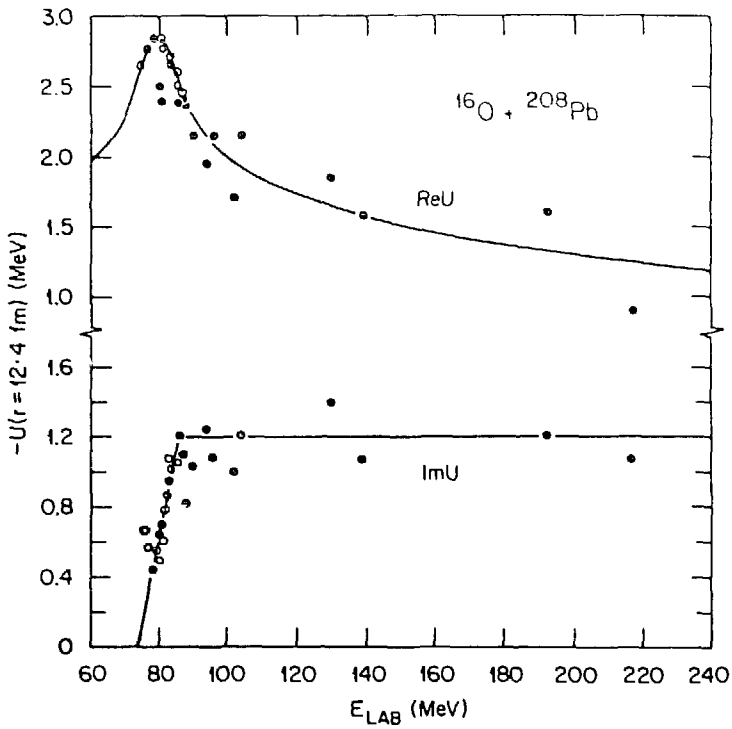

Fig. 1. Optical potential strengths.[2)]

extensive, explicit CC calculations for $^{16}O + ^{208}Pb$ which reproduce the observed elastic scattering (Figs. 3 and 4). Effective real potential corrections ("polarization potentials") have been extracted from these calculations (Fig. 5) and agree with the "anomaly" in Fig. 1. In this case, couplings to inelastic and transfer channels are of comparable importance. Qualitatively, the collision happens "suddenly" at high energies and mainly results in absorption from the elastic channel, whereas at energies near and below the barrier the processes are more adiabatic (virtual excitations) and give a real polarization potential.

Such CC calculations are complicated and specific to each system. A more general, but more implicit, approach includes all the CC dispersive effects "exactly" by using a dispersion relation[1,6)] between V(E) and W(E). This ensures that, if the absorption varies in the way just described, there will be a corresponding anomaly in the real potential. Thus it should be a universal phenomenon.

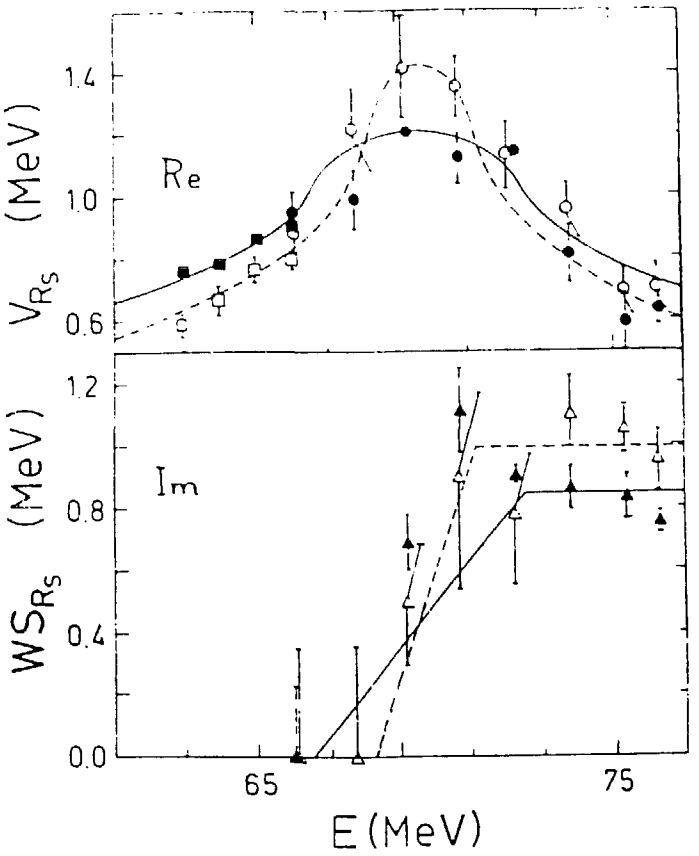

Fig. 2. Potentials strengths for ^{16}O + ^{144}Sm elastic scattering and fusion.[3)]

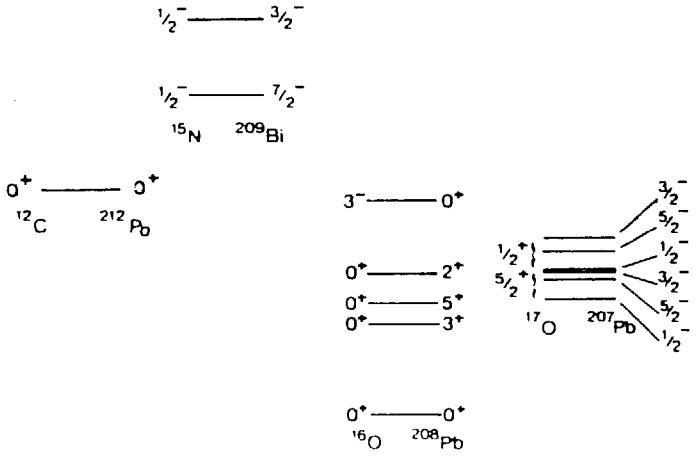

Fig. 3. Couplings for ^{16}O + ^{208}Pb.[4)]

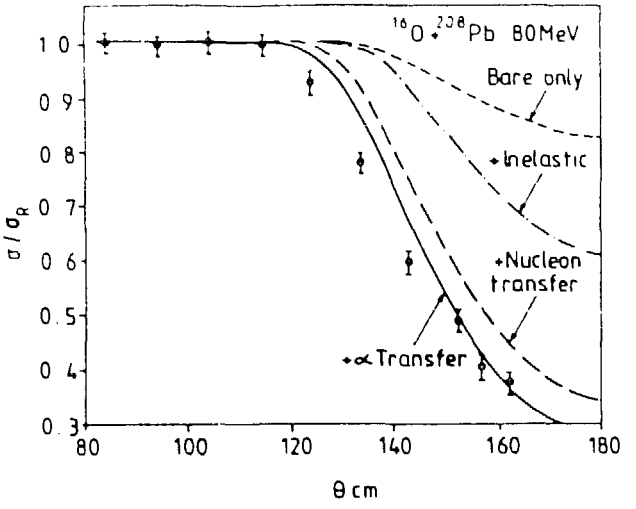

Fig. 4. Elastic scattering from CC calculations.[4]

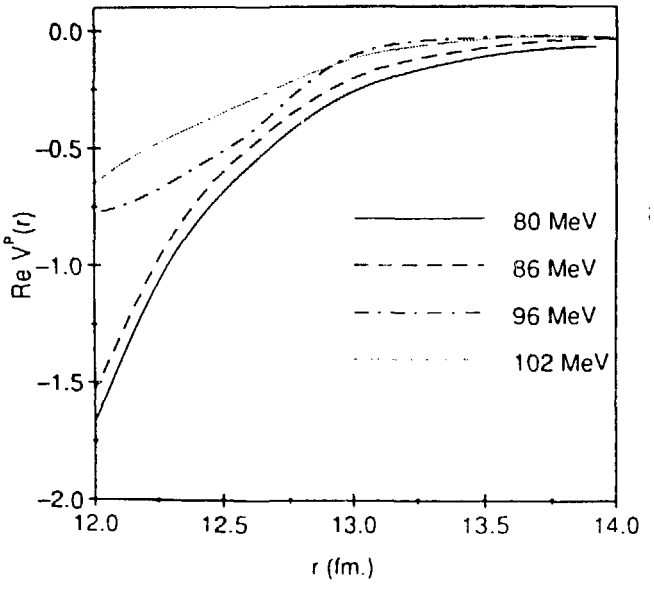

Fig. 5. Local polarization potentials[4] for $^{16}O + ^{208}Pb$.

1.2 Dispersion Relations

1.2.1 Elastic scattering. Although dispersion relations have a long history,[7] Feshbach[8] seems to have been the first to point out their application to relate the real and imaginary parts of the optical potential as derived from the analytic properties of the propagators that appear in his reaction theory. Later, this relation was derived[9] in a time-dependent framework as a consequence of causality: a scattered wave cannot be emitted before the arrival of the incident wave. The

two derivations are equivalent.

If the real potential is written $V(E) = V_o + \Delta V(E)$, where V_o is independent of E (but may be nonlocal) and ΔV has been called a dynamical polarization potential, then the dispersion relation (DR) is

$$\Delta V(E) = \frac{P}{\pi} \int_{-\infty}^{\infty} \frac{W(E')}{E'-E} \, dE', \tag{1}$$

where P denotes principal value. (There is a complementary relation in which ΔV and W are interchanged.) We see immediately that if U is complex ($W \neq 0$), then V <u>must</u> depend upon E. Further, any localized rapid increase in $|W(E)|$ (where $W < 0$), such as we have postulated near the Coulomb barrier, <u>must</u> be accompanied by an attractive contribution to ΔV localized in that same energy region. Since the absorption described by W(E) arises from couplings to nonelastic channels, we see that $\Delta V(E)$ arises from the same source. The curves in Figs. 1 and 2 were obtained from such a DR, with the W(E) represented by straight-line segments.[6] An important feature is that $|\Delta V(E)|$ begins to decrease again as the energy is lowered further. There are some indications of this from analyses of data[10,11] (Fig. 6), but it is difficult

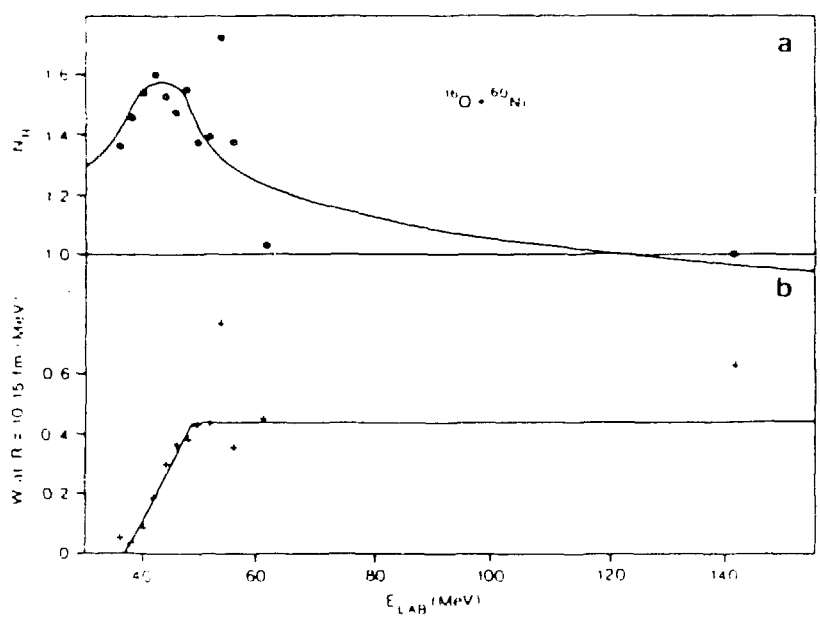

Fig. 6. Real (a) and imaginary (b) potential strengths[10] for $^{16}O + ^{60}Ni$.

to deduce optical potentials (especially the real parts) at such low energies from elastic scattering alone. More indirect evidence may come from studying fusion[3] and reaction[2] cross sections (Figs. 7 and 8).

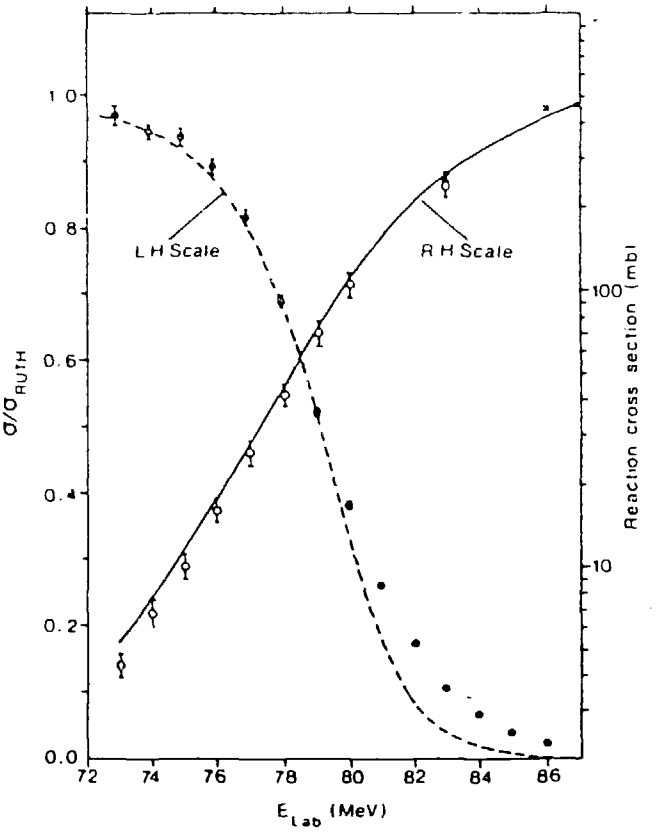

Fig. 7. Elastic scattering at 157° (LH) and reaction cross sections (RH) for $^{16}O + ^{208}Pb$.[12]

Now V_o and W, hence ΔV, are generally nonlocal,[8] but in practice model potentials are taken to be local equivalents to these. Consequently, such models will include some "spurious" energy dependence that arises from modeling the nonlocality (= momentum dependence) of the more fundamental potentials. Such a spurious E-dependence should not be included in the DR integral (1). This distinction is made routinely in treatments of nucleon potentials,[1] but for heavier ions it is usually assumed that the nonlocality correction is small and can be ignored (but see[6] for some discussion).

The DR (1) is obeyed by the potential at each position $\underline{r}$. It will also be obeyed by any moment, such as the volume integral, which may be better determined by the scattering data.[6]

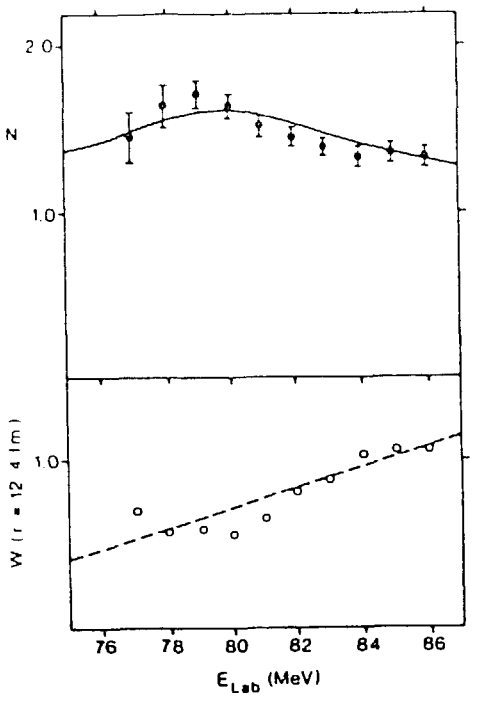

Fig. 8. Potential strengths (real: N; imaginary: W) from data in Fig. 7.[12] Curves are from the DR.

1.2.2 Nonelastic scattering. Nonelastic scattering may be treated as a limited coupled-channels problem where the one-channel optical potential is replaced by a potential matrix $U_{\beta\alpha}(E)$. Arguments parallel to those that led to Eq. (1) show[13] that each element of this matrix satisfies a corresponding DR, where now the imaginary parts $W_{\beta\alpha}(E)$ account for the loss of flux out of the explicitly coupled set of channels into all other open nonelastic channels. Since the effective number of the latter that contribute will also increase with energy at the low energies, we may anticipate a threshold anomaly (perhaps reduced in magnitude) for the real parts of the off-diagonal coupling potentials which parallels that for the diagonal optical potential.

Inelastic scattering to a 2^+ or 3^- state is particularly useful because interference with Coulomb excitation provides a sensitive indicator of the hadronic interaction in this energy region.[14,15] If the excitation is collective, it is thought appropriate to obtain the coupling interaction by deforming the ground-state optical potential. If this prescription is followed, it ensures that the coupling strength follows the elastic TA. This has been tested in at least two cases,

$^{16}O + ^{208}Pb$[14-16] and $^{16}O + ^{92}Zr$.[17] The overall TA behavior is confirmed in the former case (Fig. 9); possibly the inelastic anomaly is even stronger than the elastic one. Preliminary analysis[17] of the ^{92}Zr data shows that an anomaly is present, and also suggests the possible importance of coupling to transfer channels.

It has also been established that projectile polarization, or multistep coupling effects, are important for transfer reactions induced by $^{17}O + ^{208}Pb$ in this energy region.[12,18] In this case, the dominant intermediate step is the excitation of ^{17}O to its $1/2^+$, 0.87 MeV state. It may not be profitable to try to express this as an energy-dependent effective interaction which is exhibiting a TA, although it may be thought of in that way.

Of course, the prime example of a TA for nonelastic reactions is the enhancement of near- and sub-barrier fusion.[19] This may be represented in optical model terms, as we now discuss.

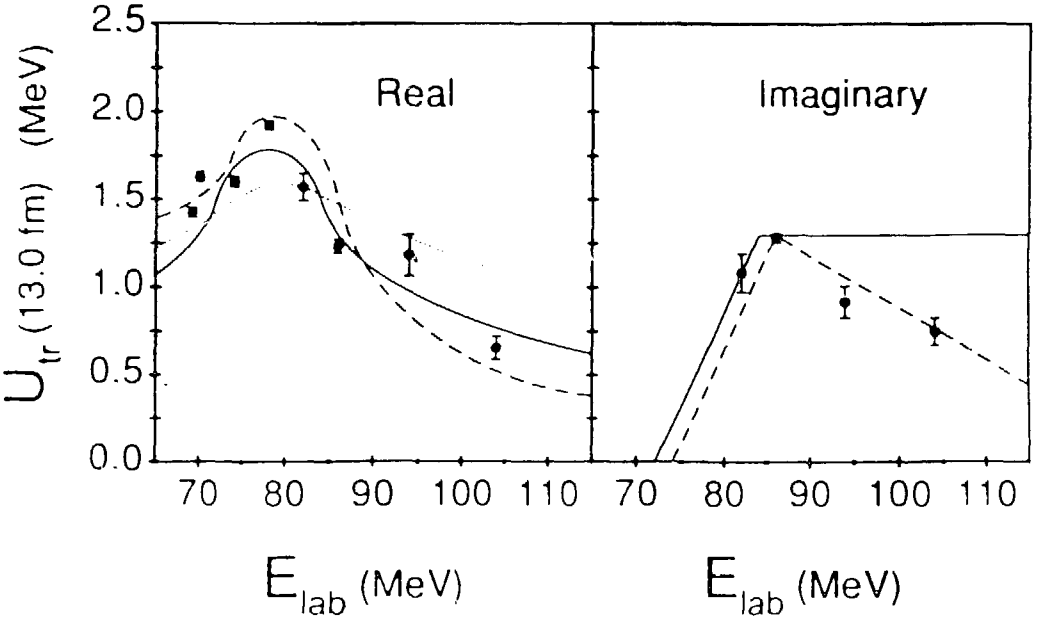

Fig. 9. Transition potentials for $^{16}O + ^{208}Pb$ (3^-) excitation.[16] Dotted line shows variation for the elastic potential (Fig. 1).

2. OPTICAL MODEL FOR FUSION

2.1 Introduction

It is now well known that sub-barrier fusion cross sections are strongly enhanced over what is expected from simple penetration of a conventional Coulomb barrier.[19] A popular way to explain this anomaly is by invoking the couplings to nonelastic channels; this can be regarded as introducing a distribution of barriers, one or more of which are lower than the uncoupled one and hence enhance the penetration.[19-22] Clearly, the fusion anomaly is another aspect of the TA seen in elastic and inelastic scattering, so we are led to examine a one-channel optical model description of fusion. Qualitatively, we can expect the increased attraction of the real nuclear potential in the barrier region to lower the barrier and ease fusion, and this motivated the first work.

We also note that a critical test of any model of heavy-ion fusion is that it reproduce correctly the spin distribution of the compound system.[23,24,27] This is equivalent, if we neglect any target or projectile spin, to the partial wave distribution $\sigma_F(L)$, where

$$\sigma_F(E) = \sum_L \sigma_F(E;L). \tag{2}$$

2.2 The Barrier Penetration Model (BPM)

The BPM assumes that fusion will occur after penetration of a conventional Coulomb barrier;[19] this is equivalent to the reaction cross section for an optical potential whose imaginary part is confined to radii inside the barrier but which is strong enough to absorb all the flux that penetrates to the interior. (Sometimes an ingoing-wave boundary condition is used[19] instead of an imaginary potential.) In actual applications, the (real) nuclear potential was taken to be independent of energy and frequently it was identified with the real part of the optical potential obtained at higher energy. It is by comparison with this model that sub-barrier fusion is said to be enhanced.

Clearly the first implication of the observed elastic TA is that the strength of the potential used in the BPM should be allowed to be energy dependent in the way found from elastic scattering,[24] and the

first applications[6] seemed to support this conjecture by producing cross section enhancements like those observed (Fig. 10). However, it

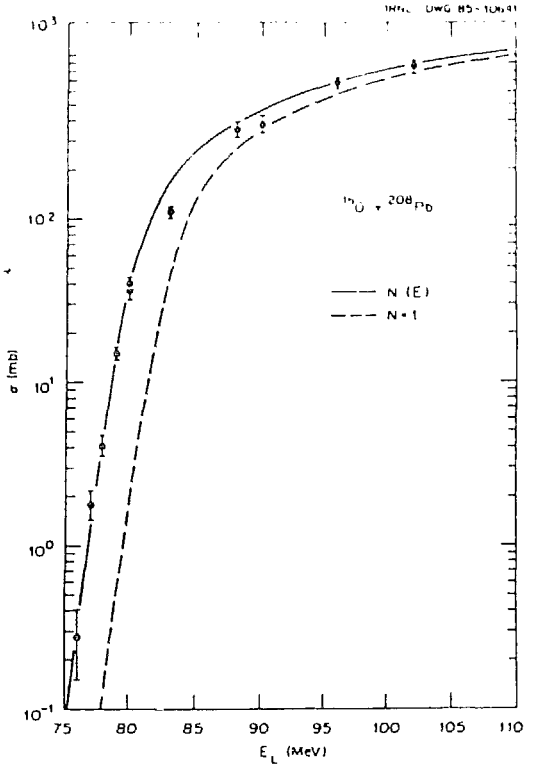

Fig. 10. Fusion cross sections[6] from BPM with a fixed (N=1) potential, and the E-dependent potential from Fig. 1, N(E).

was realized[24,27] (by comparison with CC calculations) that this was insufficient to reproduce the spin distributions (2) correctly and that at least the changes in shape of the potential across the TA[6] must be included. The discrepancy was small[24] for the case of Fig. 10, but more dramatic examples can be found[23,27] (Fig. 11).

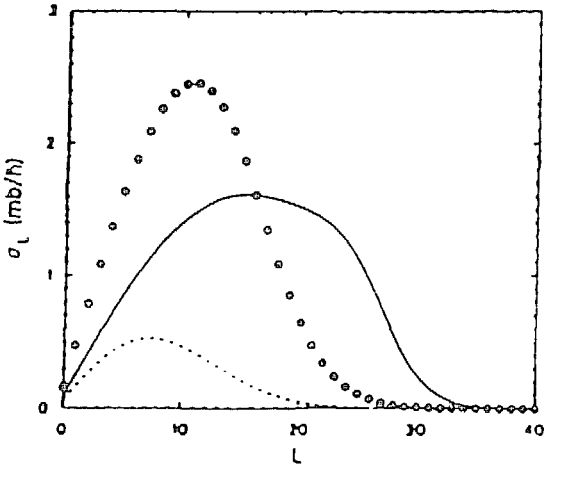

Fig. 11. Spin distributions calculated[23] for $^{40}Ar + ^{122}Sn$ at E_{cm} = 107.5 MeV. Solid: CC calculation; dashed: uncoupled; dots: uncoupled, with potential strength increased to give same σ_F as CC one.

2.3 Formal Basis of the Optical Model

To proceed further, we need to examine the formal basis of the optical model. It can be shown[25-27] that the imaginary part, W, of the optical potential U = V + iW that reproduces the elastic scattering can be divided into a piece that accounts for the fusion (F), and the remainder that describes the absorption into quasi-elastic (or direct, D) channels,

$$W(E) = W_F(E) + W_D(E). \tag{3}$$

Then the absorption cross sections are given exactly as the expectation values of the corresponding parts of W,

$$\sigma_A(E) = \sigma_F(E) + \sigma_D(E) \tag{4a}$$

$$\sigma_F(E) = -(2/\hbar v)\ \langle \chi_E^{(+)} \mid W_F(E) \mid \chi_E^{(+)} \rangle,\ \sigma_D = -(2/\hbar v)\ \langle \chi_E^{(+)} \mid W_D(E) \mid \chi_E^{(+)} \rangle, \tag{4b}$$

where the distorted waves $\chi_E^{(+)}$ are generated by the full potential U and hence include the peripheral damping due to the direct reactions.[26]

The BPM is obtained by (i) confining W_F to radii smaller than the Coulomb barrier, and (ii) neglecting W_D (and hence the peripheral damping) when generating the $\chi_E^{(+)}$. (Because of the latter condition, the BPM gives an upper limit to σ_F for a short-ranged W_F.)[27] Since, by definition, the potential U gives the elastic scattering, its real part follows the TA.

In another approach[26] Udagawa and Tamura (UT) allowed W_F to protrude into the barrier, thus providing enhanced fusion cross sections without the need for substantial changes in the real potential. This feature also broadens the spin distribution.[26-28] Initially,[26] W_F was defined by using a sharp cut-off, so that $W_F = W(r)$ for $r < R_F$, and $W_D = W(r)$ for $r > R_F$, where W(r) had a Woods-Saxon shape. Then R_F was chosen to fit the fusion cross sections. In more recent work,[29,30] W_F has been taken to have a volume (Woods-Saxon) shape (but with a sharp surface) and W_D to have a surface (Woods-Saxon-derivative) shape, with the parameters adjusted to fit simultaneously elastic and fusion data.

A striking feature of either procedure is that large values of R_F (or the corresponding radius of W_F) are obtained, values that put R_F near or beyond the radius of the top of the Coulomb barrier (typically $R_F = 1.4(A_1^{1/3} + A_2^{1/3})$). Clearly the BPM is inadequate for a W_F of this form. We also note that, in the cases of $^{32}S + {}^{58,64}Ni$ (Fig. 12), the use of a large R_F did not eliminate the need for a TA in the real and imaginary potential strengths[30] (Fig. 13). (In these fits,[30] r_F = 1.41 fm and r_D = 1.5 fm, while a_F was chosen to be small, 0.1 to 0.3 fm.)

2.4 Where Does Fusion Occur?

The results[26,28-30] of using the UT model imply that fusion is

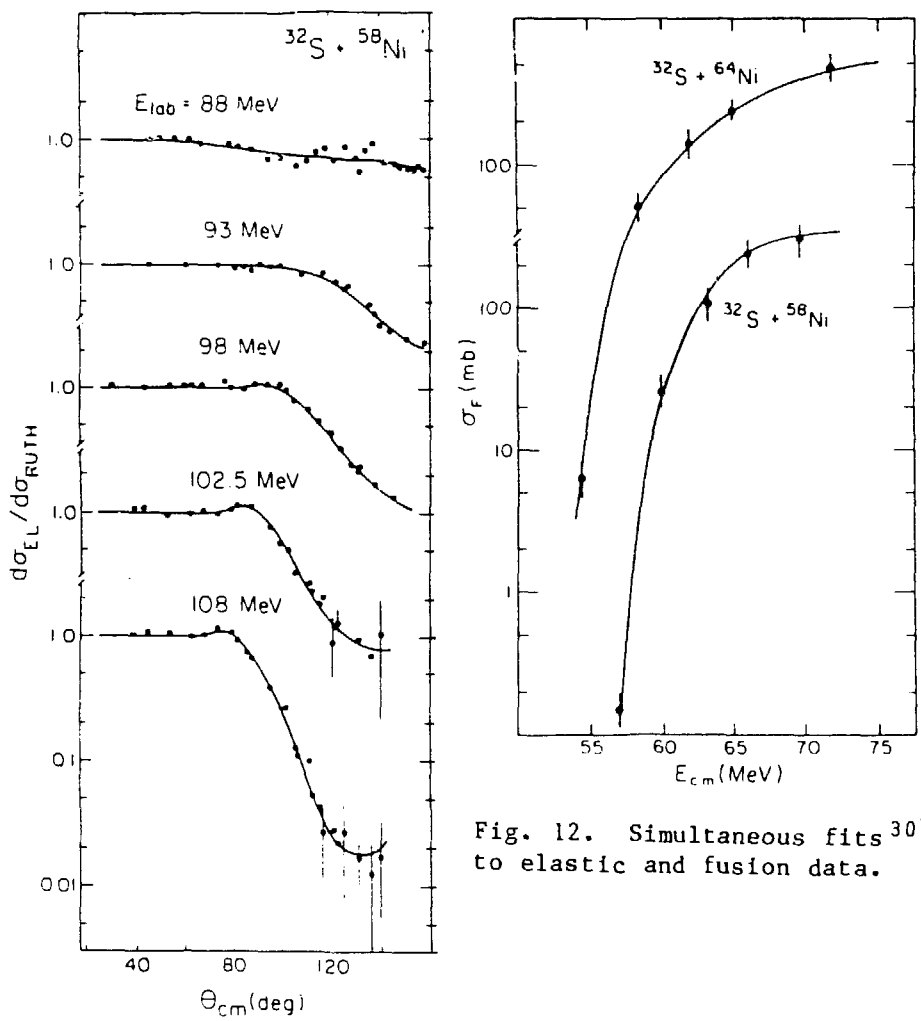

Fig. 12. Simultaneous fits[30] to elastic and fusion data.

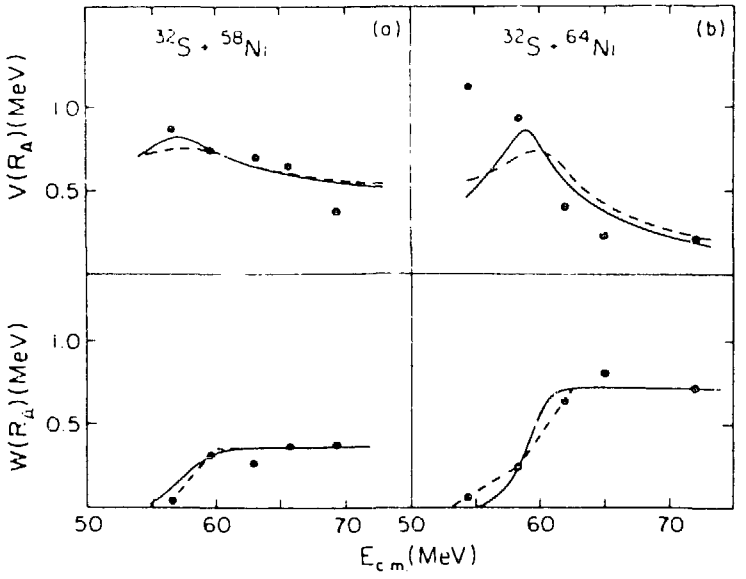

Fig. 13. Real and imaginary potential strengths[30] for data in Fig. 12.

initiated, rather suddenly, near or even beyond the top of the Coulomb barrier ($r_F \sim 1.4$ to 1.5 fm) (Fig. 14), contrary to the philosophy behind the BPM ($r_F \sim 1.0$ fm, say).

Semi-phenomenological analyses[22] of fusion for many systems, based upon a distribution of potential barriers, find a strong correlation of the enhancement with the separation energy of the least-bound neutrons of the target and/or projectile. When this is expressed as the distance of approach at which neutron flow between the ions may occur freely, it supports the notion of fusion being initiated at large radii. This work also suggests that the probability for fusion increases slowly as the nuclei approach more closely, instead of occurring rather abruptly as has been assumed in the UT optical model studies.[26] (This would correspond to using a larger diffuseness a_F for W_F than has been customary.)

We return to the formal theory of the optical potential to put this into context. The decomposition that led to (3) also shows W_F to consist of two parts,[25-27]

$$W_F(E) = W_{oF}(E) + W_{pF}(E). \tag{5}$$

The "bare" part, W_{oF}, is the imaginary potential that should appear in an explicit (and complete!) CC calculation, and describes the loss into

fusion from those "direct" channels. Customarily, it is W_{oF} that is taken to have a short range ($r_F \sim 1$ fm) or is replaced by the ingoing-wave condition inside the barrier. Then W_{pF} is the polarization contribution that results when projecting from the CC onto the elastic channel; it accounts for loss from the elastic channel due to multistep fusion, i.e. fusion that occurs after excitation into the quasielastic channels. W_D describes the loss of flux that is actually emitted into these channels, and is expected to have a surface-peaked form. The W_{pF} term can also be expected to be more peripheral, so that the sum $W_F = W_{oF} + W_{pF}$ may extend into the barrier region even if W_{oF} itself is confined to smaller radii. This could account for the large R_F values extracted in the UT approach.

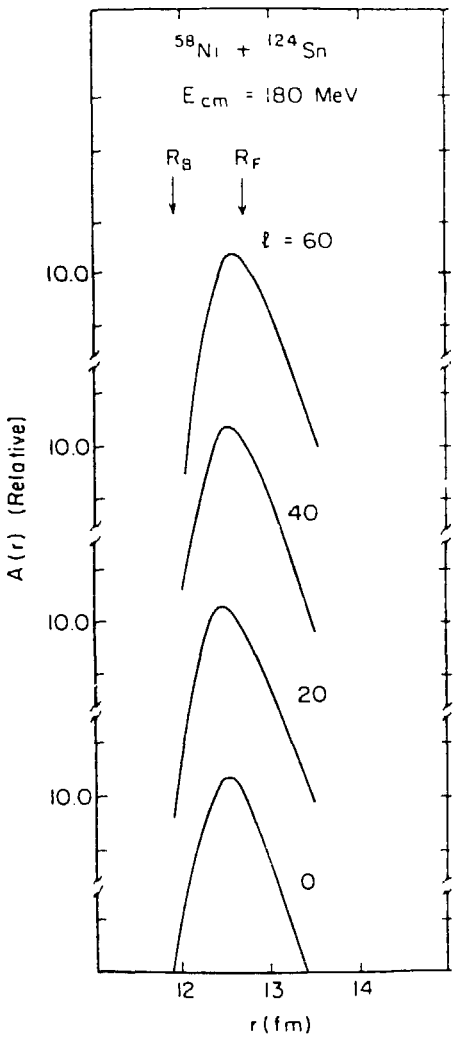

Fig. 14. Probability amplitude for fusion in UT model with $r_F = 1.42$ fm. R_B is the top of the barrier.[26]

In general, then, the imaginary optical potential should be composed of three terms, $W = W_{oF} + W_{pF} + W_D$, each energy dependent and with different radial shapes. There is no particular reason why the effects of W_{pF} should be represented by simply assigning a larger radius to W_{oF}, except a desire to economize on parameters. (The work of Stelson[22] might suggest that a large diffuseness a_F would be more appropriate.) It is hoped that some guidance may be obtained by examining the equivalent local potentials constructed from the results of large CC calculations.[4,27]

2.5 Spin Distributions

Unfortunately, at these energies the fusion cross section and elastic scattering alone are not very sensitive to such details. More empirical information can be provided by measurements of the spin distributions, $\sigma_F(L)$. As an illustration, we consider an extreme example[32] in which W_{pF} is given the same surface-peaked shape as W_D, and W_{oF} is confined inside the Coulomb barrier (r_F = 1.0 fm, a_F = 0.25 fm). The potential parameters are chosen to fit the elastic data[11] and the strength of W_{pF} adjusted to give (with W_{oF}) the fusion cross section. (The W_D term has a radius parameter r_D = 1.5 fm and diffuseness a_D = 1.0 fm.) Figure 15 compares the resulting spin distribution with that from a UT fit (with r_F = 1.41 fm, a_F = 0.2 fm) to the same data.[30] We see dramatic differences.

There are very few measurements of $\sigma_F(L)$ at near- or sub-barrier energies. Those available[31-33] are for heavier systems. They are broader than the BPM predicts (e.g., Fig. 16), and do not provide evidence for the pronounced structure, or the long tail, that our model calculation gives. This tends to confirm that taking W_{pF} and W_D to have the same shape is too extreme; one would expect, because of its multistep nature, that the W_{pF} shape would be intermediate between W_{oF} and W_D.

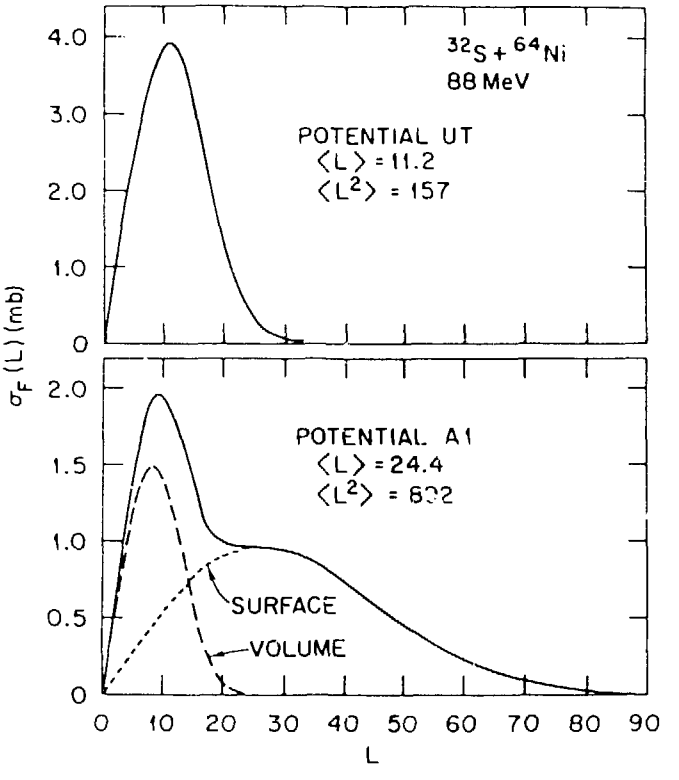

Fig. 15. Spin distributions for fusion from two potentials giving equivalent fits to the elastic data.[34]

Besides the full $\sigma_F(L)$ distribution, there are some estimates[19,35] of the moments $\langle L^n \rangle$, n = 1 or 2, from γ-ray multiplicities (n=1) or fission angular distributions (n=2). Under certain conditions, $\sigma_F(L)$ tends to a limiting shape (and the $\langle L^n \rangle$ tend to constant values) at energies well below the barrier top.[36] (One of the assumptions is that fusion occurs after tunneling through a distribution of barriers; it is not clear what happens if fusion is initiated outside the barriers.) This behavior has been inferred from recent measurements[37] on ^{12}C + ^{128}Te (Fig. 17). In this case, CC calculations seem to be in agreement with the observations. In other cases,[32,35] the inferred $\langle L^n \rangle$ remain appreciably larger than the predicted values as the energy is reduced (Fig. 18). The discrepancy is removed for at least one case[32] (Fig. 19) if the UT model is used with the large fusion radius of r_F = 1.44 fm.

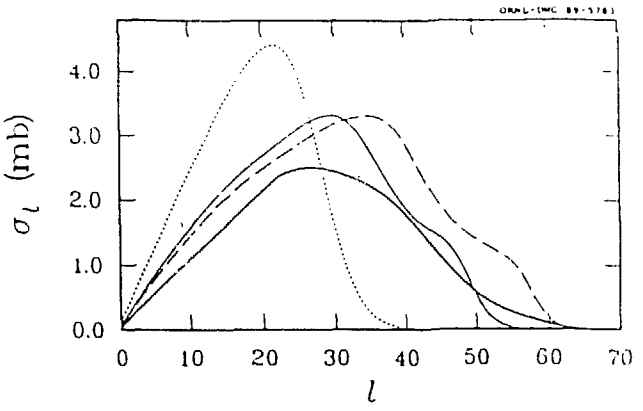

Fig. 16. Spin distributions[32] for ^{64}Ni + ^{100}Mo at 141.7 MeV. Thick line: measurements; thin line: CC calculations; dash-dot line: couplings ×1.5; dotted: uncoupled.

ACKNOWLEDGEMENTS

This research was sponsored by the Division of Nuclear Physics, U.S. Department of Energy under contract No. DE-AC05-84OR21400 with Martin Marietta Energy Systems, Inc.

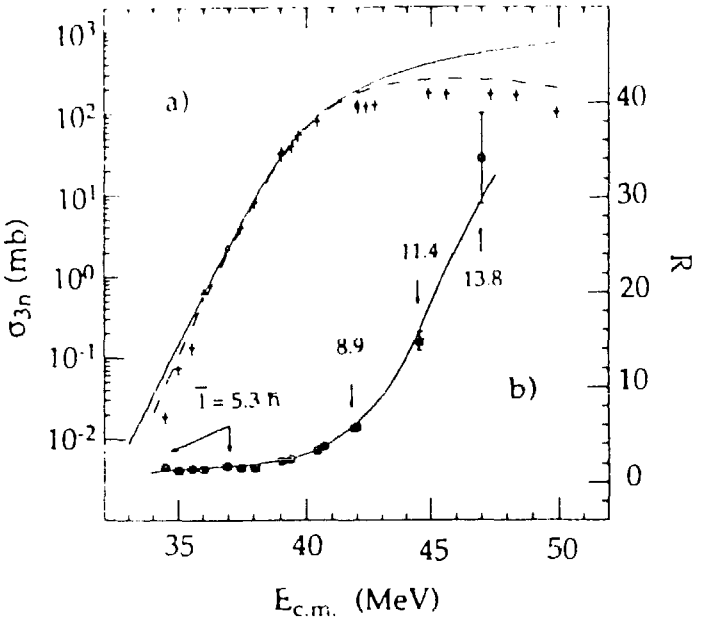

Fig. 17. (a) σ_{3n} for $^{12}C + ^{128}Te$; (b) isomer ratio for decay of ^{137}Ce and inferred ⟨L⟩ values.[37]

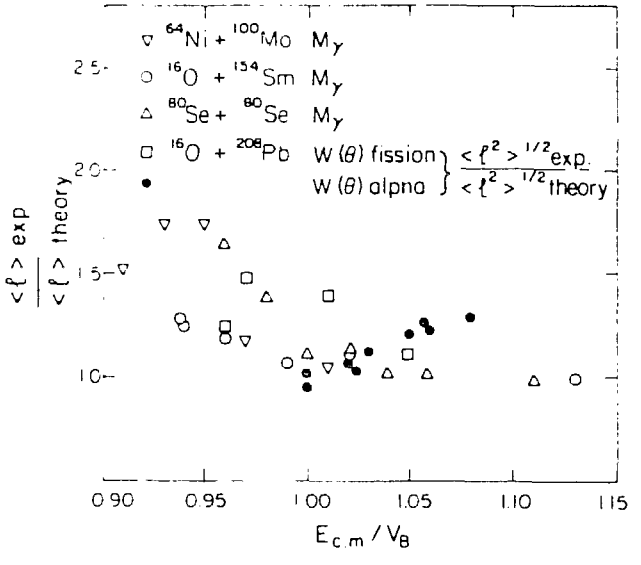

Fig. 18. Summary of ⟨L⟩ values for low-energy fusion.[35]

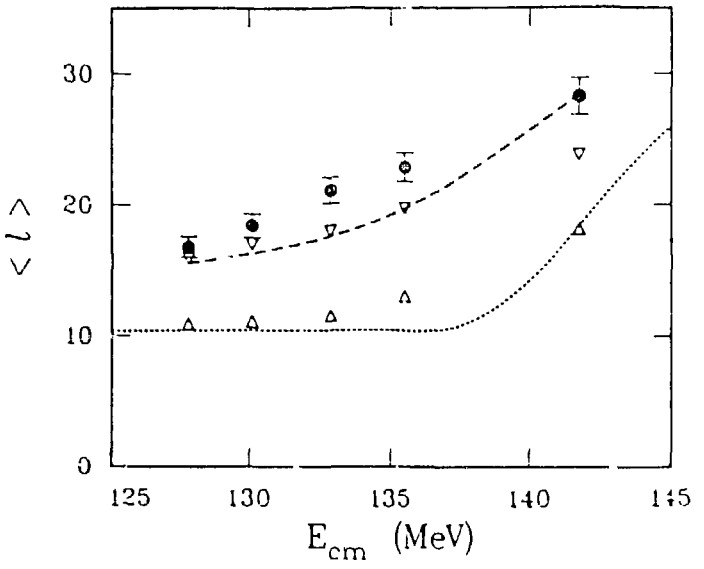

Fig. 19. Values of $\langle L \rangle$ deduced for $^{64}Ni + ^{100}Mo$.[32] Dashed curve: UT optical model; dotted curve: BPM.

3. REFERENCES

1. Mahaux, C., et al., Phys. Reports 120, 1 (1985); Nucl. Phys. A378, 205 (1982).
2. Lilley, J. S., et al., Phys. Lett. 151B, 181 (1985).
3. Abriola, D., et al., Phys. Rev. C39, 546 (1989).
4. Thompson, I. J., et al., Phys. Lett. 157B, 250 (1985); Nucl. Phys. A, to be published.
5. Pieper, S. C., et al., Phys. Lett. 162B, 43 (1985).
6. Mahaux, C., et al., Nucl. Phys. A449, 354 (1986); A456, 134 (1986).
7. Byron, F. W. and Fuller, R. W., Mathematics of Classical and Quantum Physics, Addison-Wesley (1970), p. 340.
8. Feshbach, H., Ann. Phys. (N.Y.) 5, 357 (1958).
9. Cornwall, J. M. and Ruderman, M. A., Phys. Rev. 128, 1474 (1962).
10. Fulton, B. R., et al., Phys. Lett. 162B, 55 (1985).
11. Stefanini, A. M., et al., Phys. Rev. Lett. 59, 2852 (1987) and to be published.
12. Lilley, J. S., et al., Nucl. Phys. A463, 710 (1987).
13. Satchler, G. R., Nucl. Phys. A472, 591 (1987).
14. Landowne, S., et al., Phys. Lett. 178B, 336 (1986).
15. Lim, C. S., et al., Phys. Lett. 200B, 263 (1988).
16. Lilley, J. S., et al., to be published.
17. Takagui, E. M., et al., Univ. de São Paulo, to be published.
18. Thompson, I. J., et al., Nucl. Phys. A487, 141 (1988).
19. Beckerman, M., Phys. Reports 129, 145 (1985).
20. Dasso, C. H., et al., Nucl. Phys. A407, 221 (1983).
21. Nagarajan, M. A., et al., Phys. Rev. C34, 894 (1987).
22. Stelson, P. H., Phys. Lett. 205B, 190 (1988), and to be published.
23. Dasso, C. H., et al., Phys. Lett. 217B, 25 (1989).

24. Nagarajan, M. A. and Satchler, G. R., Phys. Lett. 173B, 29 (1986).
25. Hussein, M. S., Phys. Rev. C30, 1962 (1984).
26. Udagawa, T., et al., Phys. Rev. C32, 124 (1985).
27. Satchler, G. R., et al., Ann. Phys. (N.Y.) 178, 110 (1987).
28. Kim, B. T., et al., Phys. Rev. C33, 370 (1986).
29. Hong, S. W., et al., Nucl. Phys. A491, 492 (1989).
30. Udagawa, T., et al., Phys. Rev. C39, 1840 (1989).
31. Kuhn, W., et al., Phys. Rev. Lett. 62, 1103 (1989).
32. Halbert, M. L., et al., "Frontiers of Heavy-Ion Physics", World Scientific (1981), p. 323; Phys. Rev. C, to be published.
33. Nolan, P. J., et al., Phys. Rev. Lett. 54, 2211 (1985).
34. Satchler, C. R., et al., to be published.
35. Charlop, A., et al., "Heavy-Ion Interactions Around the Coulomb Barrier", Springer-Verlag (1988), p. 157.
36. Dasso, C. H., et al., Phys. Rev. C32, 1094 (1985); Phys. Rev. Lett. 57, 1498 (1986).
37. Stokstad, R. G., et al., Phys. Rev. Lett. 62, 399 (1989).